# Combined distributed temperature and strain sensor based on Brillouin loss in an optical fiber

X. Bao, D. J. Webb, and D. A. Jackson

*Applied Optics Group, Physics Laboratory, The University, Canterbury, Kent CT2 7NR, UK*

Received July 27, 1993

We present a novel distributed sensor that utilizes the temperature and strain dependence of the frequency at which the Brillouin loss is maximized in the interaction between a cw laser and a pulsed laser. With a 22-km sensing length, a strain resolution of 20 $\mu\epsilon$ and a temperature resolution of 2 °C have been achieved with a spatial resolution of 5 m.

Long-range distributed optical fiber sensors[1-5] exploit the interaction between laser light and the fundamental energy transport mechanisms in the scattering medium. Here we report on the use of Brillouin loss[4] for a combined distributed temperature and strain sensor. Brillouin loss-based distributed sensors exploit the Brillouin interaction between pulsed and cw optical beams counterpropagating in an optical fiber. When the optical frequency of the cw beam is greater than that of the pulsed beam by an amount equal to the Brillouin frequency shift $\nu_B$ at some point in the fiber, the pulsed beam is amplified through the Brillouin interaction, and the cw beam experiences loss.

Because distributed sensors based on Brillouin scattering are sensitive to both temperature and strain, unless special precautions are taken when the fiber is deployed it will not be possible to determine whether the system is uniquely sensing a variation in temperature or strain. In a practical system it is virtually impossible to deploy the fiber such that it is not sensitive to temperature variation; however, it is feasible to install the fiber such that the effects of variation in the strain are minimized. Here we report the use of this approach to recover both measurands. Sections of the fiber were deployed such that half of its sensing length was subject to the influence of variations in both strain and temperature, whereas the other half was isolated from the effects of strain and used to determine the temperature variations of the first half of the fiber.

The experimental arrangement is illustrated in Fig. 1. Both lasers were solid-state cw diode-pumped Nd:YAG ring lasers emitting close to 1319 nm. The maximum launched power of the cw laser was ~10 mW. We could adjust the frequency of the laser by temperature tuning the cavity. An acousto-optic modulator was used to provide short optical pulses ranging in time from 50 to 500 ns. The peak launched pulsed power from the first-order diffracted beam was ~5 mW. This signal was monitored at photodetector D1 and was also used to synchronize the start of the data storage. The zero-order beam was mixed with light from the cw beam laser by directional coupler DC1 and detected with a fast (20-GHz) detector, the resultant beat frequency being monitored with a microwave spectrum analyzer.

Most of the pulsed power was launched into one end of the 22-km sensing fiber by a 90:10 coupler, DC2, whereas the cw beam was injected into the other end of the fiber by a variable ratio coupler, DC3. The cw light emerging from the sensing fiber was detected with a low-noise photoreceiver with a 125-MHz bandwidth, D2, and monitored with a storage oscilloscope. Most of the sensing fiber (22 km) remained on the original spools as supplied by the manufacturer and was subject to a constant but low-level tension. Two separate sections of the sensing fiber were placed in thermally insulated chambers. Chamber 1 contained 300 m of fiber divided into three separate 100-m lengths that were subject to different strain levels. The first 100-m fiber length was wrapped around fiber stretching unit 1, which contained two quartz cylinders, 1 and 2 (diameters 5.8 cm), separated by 0.5 m. Cylinder 1 was fixed to a translation stage, so that its position could be changed to permit stretching of this fiber section. The movement of cylinder 1 was determined with a mechanical dial gauge with 1-$\mu$m resolution. The fiber was also glued to the quartz cylinders to ensure

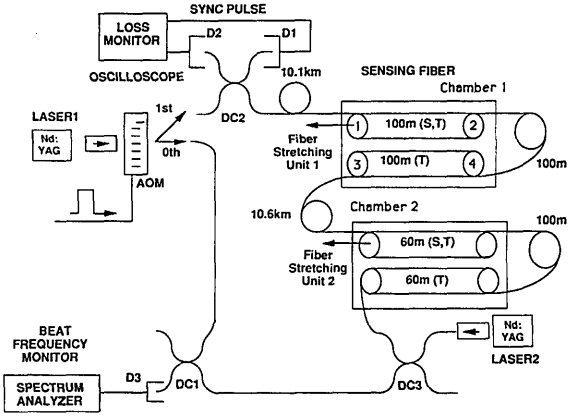


Fig. 1. Experimental arrangement: D's, photodetectors; AOM, acousto-optic modulator; DC's, directional couplers. T denotes temperature sensing, and S denotes strain sensing. Experimental details of the unit used to impose temperature and strain variations on the fibers is described in the text.

0146-9592/94/020141-03$6.00/0 

that it responded fully to the applied strain; the second 100-m fiber length was loosely coiled in a virtually tension-free condition outside the thermal chamber; the third 100 m of fiber was deployed in a similar fashion as the first 100-m length on the two other quartz cylinders, 3 and 4, with the same diameters (5.8 cm) and an initial separation of 0.5 m. The lengths of the quartz cylinders were such that they projected outside the chamber and acted as thermal insulators such that the arrangement used to strain the fiber was not affected by the temperature changes within the chambers. The second thermal chamber was arranged in a fashion similar to that of chamber 1, except that the fiber lengths in this unit were 60 m instead of 100 m. Chambers 1 and 2 were installed along the sensing fiber 10.3 and 22 km from the pulsed end, respectively.

Figure 2(a) shows one sample trace measured with the storage oscilloscope monitoring the cw beam intensity, synchronized with the launch of the pulsed beam into the fiber (time scale 50 $\mu$s/division), corresponding to 5 km per division. The pulse width is 50 ns, corresponding to a 5-m spatial resolution. This trace shows the condition in which the Brillouin loss is maximized for the fiber section 3–4 subject to a low strain at a temperature of 40 °C; a similar signal is seen from chamber 2 (38 °C), although the signal is not fully matched. Figure 2(b) is an expanded trace of that in Fig. 2(a) in the region of chamber 1. Figure 2(c) shows the case in which the beat frequency has been matched to fiber section 1–2, which is subject to an additional 100 $\mu\epsilon$ of strain at 40 °C in the same chamber. The expanded time scale for Figs. 2(b) and 2(c) is 2 $\mu$s/division, corresponding to 200 m per division. These expanded scale traces clearly show that there are three different strain regions in the chamber. To demonstrate the strain resolution of the system, we reduced the additional strain on fiber section 1–2 to 50 $\mu\epsilon$, while the temperature was maintained at 40 °C. Figure 2(d) shows the variations in the Brillouin loss signal when the beat frequency has been adjusted to maximize the loss in fiber section 1–2 at an additional 50 $\mu\epsilon$ of strain [trace (i)]. Traces (ii) and (iii) show the reduction in this signal when the additional strains were set to 20 and 0 $\mu\epsilon$, respectively. Clearly this figure shows that a change in the strain of 20 $\mu\epsilon$ can be readily detected.

Figure 3(a) shows the variation of the Brillouin frequency shift $\nu_B$ as a function of strain (measured in chamber 1) at a fixed temperature of 18 °C. The dependence of the Brillouin frequency shift on additional strain is seen to be linear. From these data and similar results measured at 22 km, the root-mean-square deviations from the best straight line fit were found to be near 20 $\mu\epsilon$. From the data, the strain coefficient of the Brillouin frequency shift was determined to be 5.4 ± 0.7 MHz per 100 $\mu\epsilon$, which agrees with the results of Kurashima *et al.*[5] According to these experimental data, we claim that the strain resolution of our system is ±20 $\mu\epsilon$.

Figure 3(b) is a plot of the laser beat frequency needed to maximize the Brillouin loss in chamber 1 as a function of temperature for fiber section 3–4. Since this part of the fiber was initially wound on the two 5.8-cm-diameter quartz cylinders at 22 °C, there was an initial winding tension such that the matched frequency $\nu_{B,\text{total}}$ corresponded to $\nu_{B,\text{strain}} + \nu_{B,T}$, where $\nu_{B,\text{strain}}$ is the Brillouin shift caused by the initial tension and $\nu_{B,T}$ is the frequency shift that is due to the temperature. The parameter $\nu_{B,T}$ can be found from the temperature measurement when the fiber is in a tension-free condition ($\nu_{B,T} = 1.2 \pm 0.2$ MHz/°C).[3] Hence as $\nu_{B,T}$ is known, then $\nu_{B,\text{strain}} = \nu_{B,\text{total}} - \nu_{B,T}$ can be found. For optimization of the Brillouin loss in an unstrained length of fiber, the initial strain in section 1–2 was found to be ~20 $\mu\epsilon$. When the oven temperature is increased, the fiber expands, and this tension will be reduced. Hence the Brillouin frequency shift needs to be corrected for this effect. The change in strain is $\sim\alpha_1 T$, where $\alpha_1$ is the thermal expansion coefficient for $GeO_2$-doped/pure-silica cladding single-mode fiber and $\alpha_1 \sim 0.62 \times 10^{-6}$/°C. For a temperature change of 60 °C, $\alpha_1 T = 37$ $\mu\epsilon$, which is equivalent to a frequency change of 2 MHz, which from Fig. 3(b) corresponds to total temperature change of 1.5 °C. Thus the maximum error, which occurs at $T = 82$ °C (for the experiment reported here) as a result of the thermally induced variation of the fiber strain, is ~2 °C.

Figure 4 shows the variation of the Brillouin frequency shift as a function of additional strain applied to fiber section 1–2 in chamber 1 at different temperatures. As can be seen from the figure, the Brillouin frequency shift with strain has a linear relation for all temperatures investigated, and the

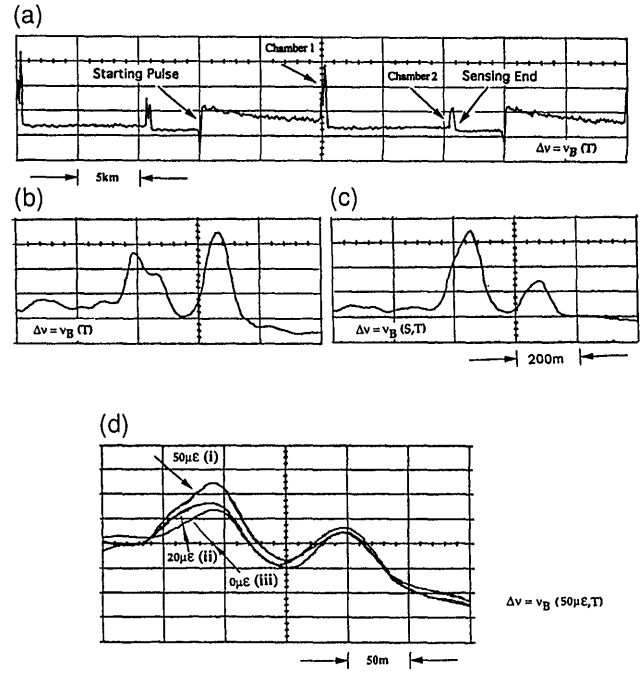


Fig. 2. Oscilloscope traces showing cw beam intensity monitored at photodetector D2, with the cw frequency set to maximize the Brillouin loss in various sections of the fiber in chamber 1 for different environmental conditions: (a) temperature 40 °C, time scale 50 $\mu$s/division; (b) fiber section 3–4 at a temperature of 40 °C; time scale 2 $\mu$s/division; (c) fiber section 1–2 at strain of 100 $\mu\epsilon$ at 40 °C; time scale 2 $\mu$s/division; (d) fiber section 1–2 strain of 50 $\mu\epsilon$ at 40 °C; time scale 0.5 $\mu$s/division.

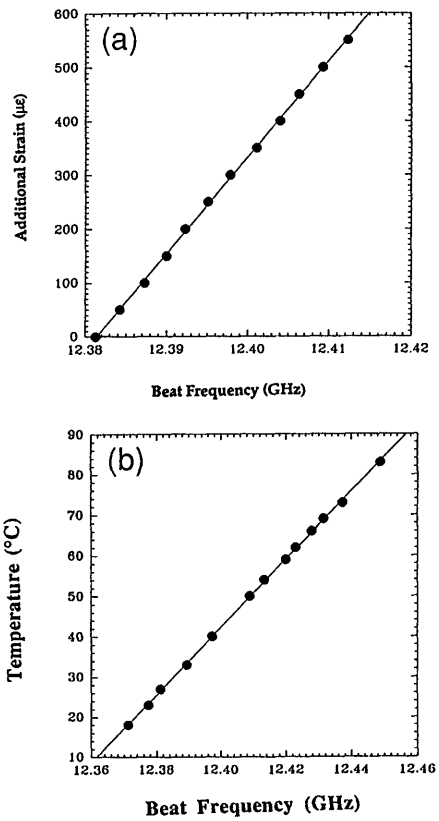


Fig. 3. Laser beat frequency giving maximum Brillouin loss for the fibers: (a) in fiber stretching unit 1 as a function of additional strain at a temperature of 18 °C, (b) in chamber 1 as a function of different temperatures at very low strain.

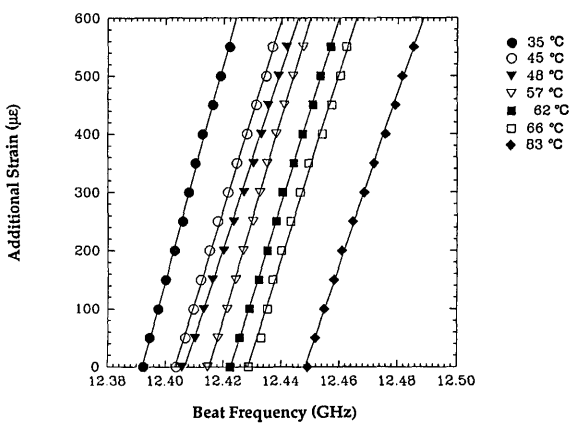


Fig. 4. Laser beat frequency giving maximum Brillouin loss for the fibers in fiber stretching unit 1 as a function of additional strain at different chamber 1 temperatures.

average strain coefficient (the slope of the straight line) is 5.7 ± 0.4 MHz per 100 $\mu\epsilon$ for the temperature range investigated (18–82 °C). This average value is slightly higher than the value measured at 18 °C, but it is within measurement errors of the system.

To use the system to measure both temperature and strain at a specific location, one will have to deploy the fiber such that the first half of the sensing is tightly bonded to the structure to be monitored; hence it will instantaneously sense both temperature and strain. The second half of the fiber will be colocated and deployed such that the effects of structural changes on the fiber are minimized, permitting the temperatures of both fiber sections to be determined.

Given that the calibration curves of Figs. 3(b) and 4 have been measured for a specific fiber and that the fiber is uniform, it is now possible to determine both the temperature and the strain of any specified location along the fiber by the following procedure. Step 1 is to measure the Brillouin frequency corresponding to the maximum Brillouin loss at the specified location in the fiber section sensitive only to temperature change and then use the Brillouin frequency to temperature coefficient from Fig. 3(b) to determine the temperature. A similar procedure is required for step 2, in which the Brillouin loss is maximized for the colocated fiber section sensitive to both temperature and strain.

The data presented in Fig. 4 are then used to deduce the strain. As it is feasible to measure only the strain-versus-frequency shift curve for a finite number of temperatures, some form of extrapolation is required. One approach is to assume that the slope of the frequency-versus-strain curve is independent of temperature; hence, from the measured value of the maximized Brillouin loss frequency at zero additional strain and the value of the temperature acquired from step 1, the strain can be obtained. The more accurate procedure would be (as indicated in Fig. 4) to measure the actual additional strain-versus-frequency curves for a large number of temperatures and then extrapolate over a smaller range—this would give a better accuracy.

To summarize, we have realized a combined distributed temperature and strain sensor based on Brillouin loss that has a 22-km sensing length with a 20-$\mu\epsilon$ resolution and 2 °C temperature resolution combined with a spatial resolution of 5 m. For this sensor to be used in a practical application, it will be necessary to deploy it such that half the sensor detects temperature and strain while the other half senses temperature, giving a sensor with a length equal to half the physical length of the fiber. It is envisaged that this sensor could be used to monitor stress levels continuously in major installations such as dams, nuclear reactors, oil pipelines, and buildings.

The authors gratefully acknowledge the financial support of the UK Science and Engineering Research Council through the Optoelectronics Interdisciplinary Research Centre, Southampton, UK.

## References

1. J. P. Dakin, D. J. Partt, G. W. Bibby, and J. N. Ross, Electron. Lett. **21,** 569 (1985).
2. T. Kurashima, T. Horiguchi, and M. Tateda, Opt. Lett. **15,** 1038 (1990).
3. X. Bao, D. J. Webb, and D. A. Jackson, Opt. Lett. **18,** 552 (1993).
4. X. Bao, D. J. Webb, and D. A. Jackson, in *Proceedings of the Ninth International Conference on Optical Fiber Sensors* (Associazione Elettrotecnica ed Elettronica Italiana, Firenze, Italy, 1993), postdeadline paper 3.
5. T. Kurashima, T. Horiguchi, and M. Tateda, IEEE Photon. Technol. Lett. **2,** 352 (1990).